A remote sensing contribution to hydrologic modelling in arid and inaccessible watersheds, Pishin Lora basin, Pakistan

Article *in* Hydrological Processes · January 2012

DOI: 10.1002/hyp.8114

CITATIONS
9

READS
244

7 authors, including:

Zhanay Sagintayev
Nazarbayev University
37 PUBLICATIONS **134** CITATIONS
SEE PROFILE

Mohamed Sultan
Western Michigan University
332 PUBLICATIONS **2,679** CITATIONS
SEE PROFILE

Shuhab D Khan
University of Houston
101 PUBLICATIONS **898** CITATIONS
SEE PROFILE

Eugene Yan
Argonne National Laboratory
81 PUBLICATIONS **818** CITATIONS
SEE PROFILE

HYDROLOGICAL PROCESSES
Hydrol. Process. **26**, 85–99 (2012)
Published online 13 June 2011 in Wiley Online Library
(wileyonlinelibrary.com) DOI: 10.1002/hyp.8114

A remote sensing contribution to hydrologic modelling in arid and inaccessible watersheds, Pishin Lora basin, Pakistan

Z. Sagintayev,[1] M. Sultan,[1]* S. D. Khan,[2] S. A. Khan,[3] K. Mahmood,[3] E. Yan,[4] A. Milewski,[1] and P. Marsala[1]

[1] *Department of Geosciences, Western Michigan University, Kalamazoo, MI, USA*
[2] *Department of Earth and Atmospheric Sciences, University of Houston, Houston, TX, USA*
[3] *National Center of Excellence in Mineralogy, University of Balochistan, Quetta, Pakistan*
[4] *Environmental Science Division, Argonne National Laboratory, Chicago, IL, USA*

Abstract:

The lack of adequate field measurements often hampers the construction and calibration of rainfall-runoff models over many of the world's watersheds. We adopted methodologies that rely heavily on readily available remote sensing datasets as viable alternatives for assessing, managing, and modelling of such remote and inadequately gauged regions. The Soil and Water Assessment Tool was selected for continuous (1998–2005) rainfall-runoff modelling of one such area, the northeast part of the Pishin Lora basin (NEPL). Input to the model included satellite-based Tropical Rainfall Measuring Mission precipitation data, and modelled runoff was calibrated against satellite-based observations, the latter included: (i) monthly estimates of the water volumes impounded by the Khushdil Khan (latitude 30°40′N, longitude 67°40′E), and the Kara Lora (latitude 30°34′N, longitude 66°52′E) reservoirs, and (ii) inferred wet *versus* dry conditions in streams across the NEPL. Calibrations were also conducted against observed flow reported from the Burj Aziz Khan station at the NEPL outlet (latitude 30°20′N; longitude 66°35′E). Model simulations indicate that (i) average annual precipitation (1998–2005), runoff and recharge in the NEPL are 1300×10^6 m^3, 148×10^6 m^3, and 361×10^6 m^3, respectively; (ii) within the NEPL watershed, precipitation and runoff are high for the northeast (precipitation: 194 mm/year; runoff: 38×10^6 m^3/year) and northwest (134 mm/year; 26×10^6 m^3/year) basins compared to the southern basin (124 mm/year; 8×10^6 m^3/year); and (3) construction of delay action dams in the northeast and northwest basins could increase recharge from 361×10^6 m^3/year up to 432×10^6 m^3/year and achieve sustainable extraction. The adopted methodologies are not a substitute for traditional approaches, but they could provide first-order estimates for rainfall, runoff, and recharge in the arid and semi-arid parts of the world that are inaccessible and/or lack adequate coverage with field data. Copyright © 2011 John Wiley & Sons, Ltd.

KEY WORDS Pishin Lora basin; Balochistan; Pakistan; continuous rainfall-runoff model; soil water assessment tool; remote sensing

Received 20 September 2010; Accepted 28 March 2011

INTRODUCTION

Balochistan is the largest province in Pakistan, yet it has the smallest number of people per unit area. This is largely because of its arid to semi-arid conditions (rainfall: ∼100 mm/year) and the paucity of its water resources. In recent years, the indiscriminate and unplanned use of groundwater resources in Balochistan has led to water shortages, unsustainable overexploitation of groundwater, and progressive deterioration in groundwater quality and quantity (TCI *et al.*, 2004). Water shortages in the area were exemplified by the recent drought conditions that affected the area, causing population migration from rural to urban centres, and by war-related migrations from neighbouring Afghanistan. These factors contributed to a dramatic rise in the local population of the Quetta Valley in general, and the city of Quetta in particular. Quetta Valley is part of the Pishin Lora watershed, and the city of Quetta is the capital of the Balochistan province (Figure 1); both areas are bearing the brunt of the population migration (IWRM, 2004).

Flooding events are rare but can be catastrophic. Large watersheds in mountainous areas can channel vast amounts of water into a limited number of main channels downstream, causing extreme flooding. According to the Government of Balochistan, in the past decade or so, drought-flooding cataclysms affected 85% of the Balochistan population; over 2 million people migrated, 75% of the livestock died, and three major dams crashed in the flood of 2005 alone (RedCross, 2005; Majeed and Khan, 2008). Our research addresses the urgent need to assess and develop the Pishin Lora basin groundwater resources, as well as the general deficiency in understanding the hydrogeologic setting, namely the temporal and spatial partitioning of precipitation in the area; one of our goals is to develop scenarios for sustainable water extraction in the Pishin Lora basin.

We adopted a catchment-based continuous (1998–2005) rainfall-runoff model for the northeast part of the Pishin Lora basin (NEPL) watershed using the Soil and Water Assessment Tool (SWAT) (Arnold and Fohrer,

* Correspondence to: M. Sultan, Department of Geosciences, Western Michigan University, Kalamazoo, MI, USA.
E-mail: mohamed.sultan@wmich.edu

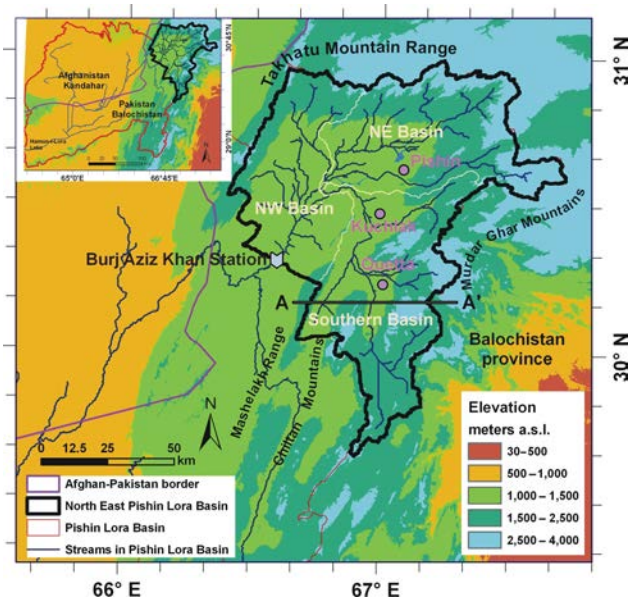

Figure 1. Location, extent, and elevations for the Pishin Lora basin shown in the inset in the upper left corner (outlined by red lines), the NEPL watershed (outlined by thick black lines), the NE, NW, and Southern basins inside within the NEPL (outlined by white lines). Also shown are stream networks in Pishin Lora and in the NEPL (blue lines), Afghanistan–Pakistan's border (purple line), main cities (Pishin, Kuchlak, and Quetta), Burj Aziz Khan discharge station, mountain ranges, and the location of cross-section A–A′ displayed in Figure 2

2005; Arnold *et al*., 1998). The NEPL is a large and important watershed that covers an area of 8500 km^2; it is subdivided into three main basins, the southern, northeast (NE), and northwest (NW) basins (Figure 1), with the majority of the precipitation occurring over the NE and NW basins. The NEPL was selected for the following reasons: (i) it has the highest elevations (up to 3500 m) in the Pishin Lora basin (Figure 1), and is thus more likely to receive substantial amounts of precipitation (Kazmi *et al*., 2003), (ii) the Quetta Valley in general, and the city in particular, are the most popular destinations for the waves of immigrants, and (iii) stream flow data needed for calibration purposes are available for the Burj Aziz Khan station (latitude 30°20′; longitude 66°35′) on the West end outlet on the NEPL (Figure 1).

Given the paucity of monitoring systems (e.g. rain gauges, stream flow gauges), and the difficulty in accessing the areas of investigation because of ongoing security problems, we adopt an approach that relies heavily on observations extracted from readily available remote sensing datasets. Remotely sensed data (e.g. precipitation from TRMM) were used as inputs to the model; the model outputs (e.g. runoff) were calibrated against observations (e.g. reservoir volume, wet *versus* dry streams) extracted from temporal satellite imagery. The methodologies adopted here are similar to earlier attempts (Ottle *et al*., 1989; Schultz, 1993; Droogers and Bastiaanssen, 2002; Miller *et al*., 2002; Milewski *et al*., 2009a; Milewski *et al*., 2009b) in that they utilize remotely acquired parameters (e.g. basin characteristics) as inputs to the hydrologic model, but attempt to utilize remote sensing data to calibrate it as well. The adopted methodologies could potentially be applied to many of the world's watersheds that are inaccessible and lack adequate field monitoring datasets.

SITE DESCRIPTION

The Pishin Lora basin is a landlocked watershed located on the border of two provinces, Balochistan (Pakistan) and Kandahar (Afghanistan). The upstream areas are generally in the eastern highlands in Pakistan; the streams cross into Afghanistan, then flow back into Pakistan and feed the salty Hamun-i-Lora Lake (21 km^2, 1·1 km above mean sea level [AMSL]) in Balochistan (Figure 1). The area of the Pishin Lora is 61 300 km^2 and that of the NEPL is 8470 km^2, approximately 15% of the Pishin Lora basin (Figure 1).

The geologic and structural history of the study area and its surroundings is complex, as it represents the western edge of the collision zone between the Indo-Pakistan and Eurasian plates. This collision consumed the Tethys Ocean that extended in the NEPL and surroundings (HSC, 1961a). It has been suggested that in this area the Indian plate did not collide with the Afghan block until the Late Pliocene (Treloar and Izatt, 1993). The study area is predominantly composed of sedimentary sequences reaching up to 11 km in thickness. The sequence is subdivided into three main groups: (i) the lower part is composed of a marine carbonate sequence, approximately 5 km thick, that was deposited before the collision; (ii) the middle section is composed predominantly of thick (∼3 km) sequences of mudrock with subordinate amounts of sandstone and carbonate that were deposited during or before the collision; and (iii) the upper sequences are composed of thick (∼3 km) clastic sediments that were eroded from the uplifted mountains. The lower sequence in the study area is largely composed of limestone of Permian to Middle Jurassic age that belongs to the Shirinab and overlying Chiltan formations. These sequences accumulated on a shallow marine shelf along the coast of Gondwana as early as the Permian period and continued to accumulate throughout the Cretaceous in a passive continental margin setting (Table I).

Two main types of aquifers are reported in the area, alluvial aquifers in the valleys and bedrock aquifers in the surrounding mountains. These two aquifers are in direct contact and are hydraulically connected (Shan, 1972; Kazmi *et al*., 2003; TCI *et al*., 2004; Halcrow and Cameous, 2008;). The majority of the wells in the study area extract water from the thick (30–900 m) alluvial deposits in the main valleys; less groundwater is being extracted from the bedrock aquifers (Kazmi *et al*., 2003; TCI *et al*., 2004).

The thickest alluvial aquifers are found in the main valleys, the Quetta, Kargaza, and Barj Azir-Ghazaband valleys (Figure 2), which are adjacent to, and running along the foothills of, the major mountain ranges in the area (e.g. Murdar Ghar, Chiltan-Takatu, and Mashelakh;

Table I. Geologic and hydrogeologic data for the Pishin Lora basin compiled from HSC (1961a), Kazmi (2003), Maidment (1993), and TCI (2004)

Lithologic units	Age	Lithology	Hydraulic conductivity SOL_K, mm/h, and soil group (A,B,C,D)	Consolidated soil types for SWAT
Unconsolidated deposit (stream-bed and sub-piedmont deposits)	Quaternary Holocene, 10 KYA–present	Silts, sands, gravels, boulders, cobbles	40 mm/h, A, alluvium	Alluvium
Bostan Formation	Quaternary Pleistocene, 2 MYA–10 KYA	Sandstone with partially consolidated clay, silt, sand, and gravel	28 mm/h, A, sandstone	Sandstone
Siwalik group	Tertiary Miocene Pliocene, 20–2 MYA	Sandstone conglomerates	28 mm/h, A, sandstone	
Gaj Formation	Tertiary Miocene, 23–20 MYA	Shale	1·9 mm/h, C, shale	Shale
Kirthar Formation	Tertiary Oligocene, 33–23 MYA	Highly fractured fossiliferous limestone	20 mm/h, A, limestone (Karstified)	Limestone
Ghazij Formation	Tertiary Eocene, 55–33 MYA	Shale interbedded with claystone, mudstone, sandstone, limestone, and conglomerate	1·9 mm/h, C, shale	Shale
Dungan Formation	Tertiary Paleocene, 65–55 MYA	Limestone karstified with subordinate marl, shale, and sandstone	20 mm/h, A, limestone (karstified)	Limestone
Bela volcanic group	Cretaceous, 145–65 MYA	Lava flows, volcanic conglomerate, volcanic breccia, mudstone	0·01 mm/h, D, igneous rock	Igneous Rock
Chiltan Formation	Jurassic, 200–145 MYA	Limestone karstified	20 mm/h, A, limestone (karstified)	Limestone
Shirinab Formation	Permian–M. Jurassic, 270–200 MYA	Bedded limestone and intercalated shale	1·9 mm/h, C, limestone	

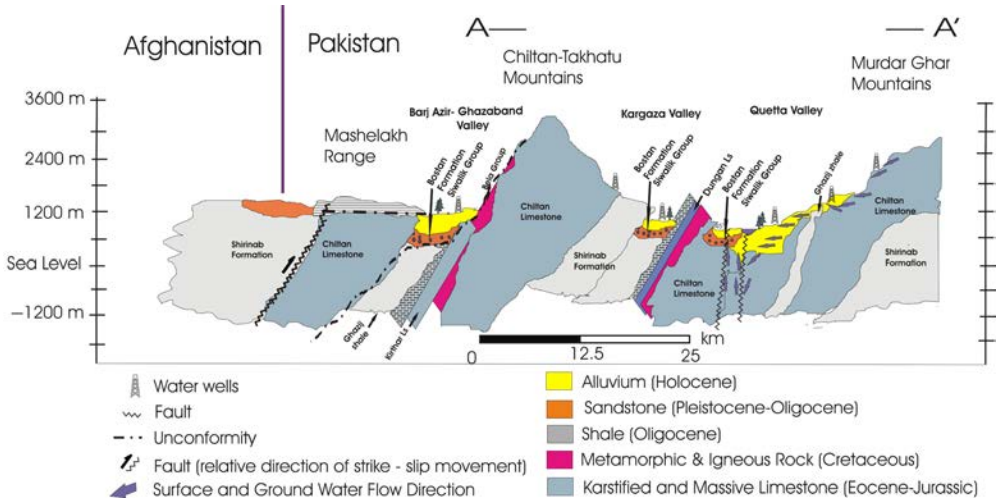

Figure 2. East-west trending cross-section A–A′ outlined in Figure 1, showing the distribution of main valleys, mountain ranges, and lithological and structural elements at depth

Figures 1 and 2). The alluvial aquifers are in contact with the underlying sandstone aquifers of the Bostan Formation and Siwalik Group. The Siwalik Group, the Bostan Formation, and the overlying unconsolidated deposits cover most of NEPL, including the valleys occupied by the Pishin Lora, Chinar N, Surhab Lora, Sariab Lora, and Karak Lora rivers and their tributaries (Aftab, 1997) (Figure 3(b)) and are largely composed of poorly cemented conglomerate and thus provide adequate recharge zones.

The hard rock aquifers are largely found in the karstified Chiltan Formation, and to a much lesser extent in the Dungan and Kirthar Formations; the distribution of groundwater in the Dungan and Kirthar Formations is apparently structurally controlled (Kazmi *et al*., 2003; TCI *et al*., 2004). The aquifer properties of the Chiltan

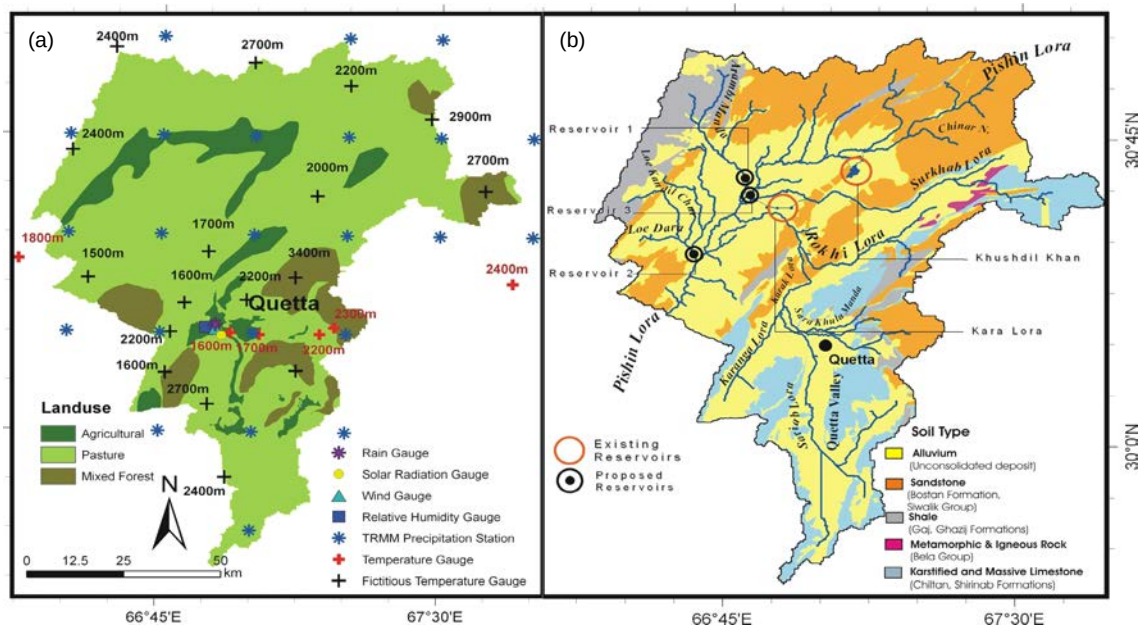

Figure 3. Distribution of land use and soil types in the NEPL. (a) Distribution of land use types, TRMM stations, climatic stations (six temperature gauges; red crosses) and their elevations, and fictitious stations (black crosses) and their elevations to enable estimation of maximum and minimum daily temperatures at these locations for modelling purposes. (b) Distribution of soil types and stream networks. Also shown are locations of the existing major reservoirs and the proposed locations for additional reservoirs

Formation and to a lesser extent the Kirthar and Dungan Formations, are enhanced by its karstified texture and its well-jointed and highly fractured nature. Numerous springs of considerable discharge were reported from these formations (Aftab, 1997; Kazmi *et al*., 2003).

Examination of the temporal and spatial distribution of precipitation, temperature, and stream flow data indicated that the amount of precipitation is quite variable from year to year, as indicated by the average annual precipitation data extracted from the Tropical Rainfall Measuring Mission (TRMM) (Simpson *et al*., 1988) (Figure 4). Figure 4 shows that in 2003 and 2005, precipitation was high, whereas precipitation from 1998 through 2002 and 2004 was negligible. The lowest temperatures (as low as $-10\,^{\circ}$C) are reported for December, January, and February (Shan, 1972; Kazmi *et al*., 2003; TCI *et al*., 2004; PMD, 2010), the time period during which snow accumulates on the mountains (e.g. Chiltan-Takhatu and Murdar Ghar; Figure 2). In the spring, snow starts melting slowly and percolates down as overflow and interflow from the highlands of the Murdar Ghar and Chiltan-Takhatu Mountains toward the interleaving valleys, including Quetta Valley (Figure 2).

A common practice in the area is to dam the melted snow coming off the highlands to increase infiltration, and recharge the alluvial aquifers in the area. Of the 292 delay action/storage dams constructed in Balochistan, 127 were implemented in the Pishin Lora (Halcrow and Cameous, 2008). The majority of the constructed dams are quite small, as are the reservoirs formed by the impounded runoff (area $<0{\cdot}01$ km^2). Only two major reservoirs built near the cities of Pishin and Kuchlak, the Khushdil Khan (latitude 30°40′N, longitude 67°40′E) and the Kara Lora (latitude 30°34′N, longitude 66°52′E) reservoirs (Figures 1, 3(b)), were recognisable in Landsat TM scenes. The former collects runoff from the Chinar N. River and from the Pishin Lora Rivers; the latter is from the Surkhab Lora River (Figure 3(b)).

MODEL CONSTRUCTION AND CALIBRATION; REMOTE SENSING CONTRIBUTIONS

Model framework

A continuous rainfall-runoff model for the NEPL was constructed within the SWAT framework to simulate the hydrologic processes using its physically based formulations. SWAT is a semi-distributed continuous watershed simulator that computes long-term water balance over large basins using daily time steps. SWAT was selected because it is a continuous model, allowing rainfall-runoff and groundwater-recharge estimates to be made over extended periods of time; it is also compatible with Geographic Information System (GIS) data formats, allowing us to import the existing GIS databases for the NEPL into the model. Because SWAT allows water balance to be calculated for each soil/land use type, defined as hydrologic response units (HRUs) (Neitsch *et al*., 2002), the NEPL was divided into a number of sub-basins, which were further subdivided into HRUs. The water balance of each HRU, including snow pack/melting, surface runoff/infiltration, evapotranspiration, groundwater recharge was calculated through four water storage bodies (snow, soil profile, shallow aquifer, and deep aquifer). The areal coverage of snow over each of the HRUs was defined using a linear areal depletion curve (Anderson *et al*., 1976); the curve was also used to estimate the seasonal growth and recession of snow pack and to determine snowmelt. A modified Soil Conservation Service

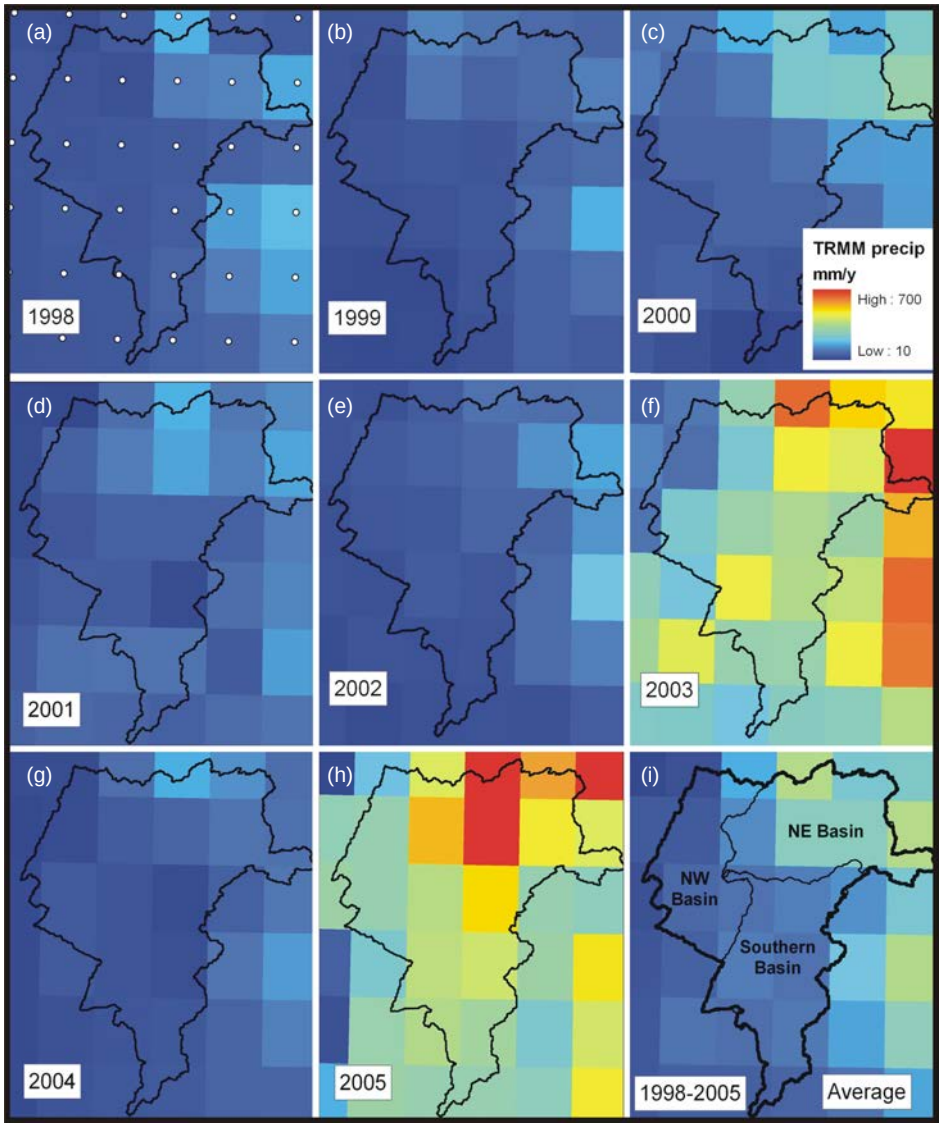

Figure 4. Annual precipitation extracted from 3-hourly TRMM precipitation data over NEPL and surroundings for years 1998 through 2005 ((a)–(h)) showing large variations in precipitation amounts. (i) Average annual precipitation (1998–2005). Also shown are locations of TRMM stations (white circles; (a)) and the outlines of the major basins within NEPL. The highest precipitation rates are observed in the northeastern part of the NEPL

(SCS) curve number (CN) method (SCS, 1972), adjusted according to soil moisture conditions, was used to calculate direct surface runoff. The Penman-Monteith method (Monteith, 1981) was used to estimate evaporation on bare soils and evapotranspiration on vegetated areas. Flows generated from each HRU were then summed and routed through channels, ponds, and/or reservoirs to the outlets of the watershed (Srinivasan *et al*., 1998; DiLuzio *et al*., 2001). The construction and calibration of the model was facilitated by the development of a GIS database to host all relevant datasets for the NEPL basin; these data served as input for the SWAT rainfall-runoff model. The ArcGIS 9·3 interface for SWAT2005 software (DiLuzio *et al*., 2001) was used for data input.

Data collection

A large number of digital datasets were generated for modelling and calibration purposes: (i) A digital elevation model (DEM; spatial resolution of 90 m) was constructed from the Shuttle Radar Topography Mission (SRTM) data, (ii) Temporal and spatial distributions of temperature, relative humidity, wind speed, and solar radiation were generated from the available climatic stations, (iii) Temporal (1998–2005) and spatial daily distribution maps for precipitation and snow accumulation were generated 3-hourly, collecting data once every 3 h, TRMM (3B42.v6) precipitation data (spatial resolution: $0{\cdot}25^\circ \times 0{\cdot}25^\circ$); data were extracted from the National Aeronautics and Space Administration (NASA) Distributed Active Archive Center (DAAC), (iv) The spatial distribution of land use and soil types was extracted from published data (HSC, 1961b; Abbas *et al*., 1987; IIASES, 1992; Mirza, 1995; ACO, 2004), (v) Daily distribution maps for clouds were constructed for verification of TRMM-derived precipitation events (Milewski *et al*., 2009b); data were extracted from the Advanced Very High Resolution Radiometer (AVHRR) scenes acquired (2003–2005) from the National Oceanic

and Atmospheric Administration Comprehensive Large Array-Data Stewardship System (NOAA CLASS, spatial resolution: 1·09 km) and from Moderate Resolution Imaging Spectroradiometer (MODIS) scenes (spatial resolution: 250 m), (vi) Landsat Thematic Mapper (Landsat TM) scenes (spatial resolution: 28·5 m) acquired (1998–2005) from the US Geological Survey (USGS) database were used to refine the DEM-derived stream networks, to extract reservoir volumes, and to examine whether streams were wet or dry.

The Remote Sensing Data Extraction Model (RESDEM) was used to preprocess large remote sensing datasets (e.g. TRMM, AVHRR). RESDEM allows users to extract user-defined subsets from the global satellite datasets and process the selected subsets in ways that unify projections, eliminate spectral variations related to differences in sun angle elevations, and verify TRMM-based precipitation events while applying verification procedure modules connected to cloud detection (Milewski *et al*., 2009b).

Digital elevation–watershed and stream delineation, and reservoir storage

The DEM mosaic covering the entire Pishin Lora watershed was used to delineate the watershed boundaries and stream network using the Topographic Parameterization (TOPAZ) program (Garbrecht and Martz, 1995). The NEPL watershed was subdivided into 104 sub-basins, with sizes ranging from 0·14 to 650 km^2 (Figure 5). Dam storage parameters (e.g. reservoir surface area and volume) were extracted on a monthly basis from temporal (1998–2005) Landsat images and SRTM data and used for calibration purposes (in a later section).

Climate datasets–temporal and spatial precipitation over watersheds

Climatic datasets were imported to evaluate the TRMM-derived precipitation data, to determine onset of snow pack growth and melting, compute evapotranspiration, and constrain runoff and groundwater contributions. We chose to extract precipitation information from the TRMM data because of the limited and uneven distribution of precipitation gauges in the study area and the general correspondence between the TRMM and the precipitation reported from the Quetta Meteorological Station. Only one precipitation data station, the Quetta Meteorological Station, is located within the NEPL, and none are located on the Takhatu Mountain Range in the north, the highlands that receive the highest amount of precipitation in the NEPL (Figures 1 and 4). For modelling purposes, precipitation extracted from TRMM data that was deposited below a threshold temperature value was classified as snowfall.

We used the data available from the Quetta Meteotological Station to evaluate the quality of the TRMM-based precipitation. A general correspondence (R^2: 0·88) was observed between the average monthly (1998–2005) precipitation measured in the field and that derived from TRMM data over the same area (Figure 6(a)). One

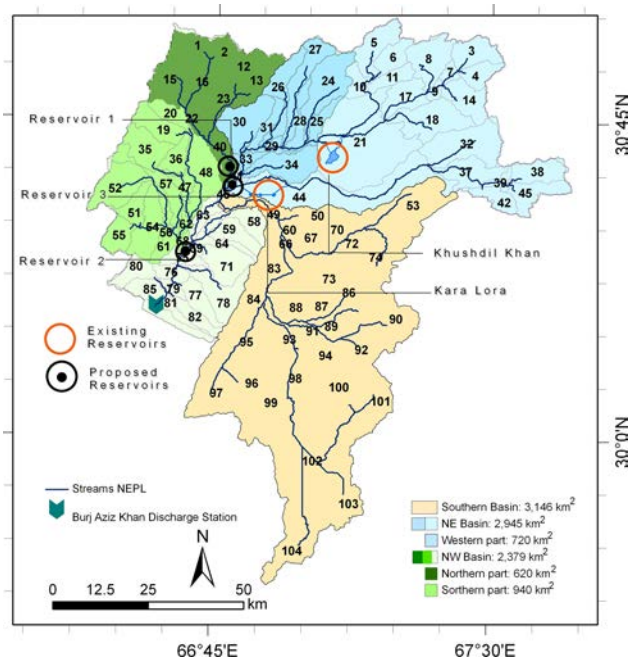

Figure 5. Distribution of major (NE, NW, and Southern basins) and minor (104) sub-basins within the NEPL watershed. Also shown are the locations of Burj Aziz Khan Discharge Station and the Khushdil Khan and Kara Lora reservoirs, in sub-basins 21 and 44, respectively, and the location of the proposed additional reservoirs: reservoir 1 (sub-basin 40), reservoir 2 (sub-basins 41), and reservoir 3 (sub-basin 68)

should not expect a 1 : 1 correspondence between TRMM and field-derived measurements because TRMM integrates observations over a large area ($0{\cdot}25^\circ \times 0{\cdot}25^\circ$), whereas rain gauges provide local measurements. The 3B42.v6 TRMM dataset was selected because it has lower false-alarm rates (FAR), higher probability of detection (POD) rates, and a greater overall critical success index (CSI) compared to the other TRMM products, including 3B42.v5 and 3B43.v5 (Chokngamwong and Chiu, 2006).

Examination of daily maximum and minimum temperatures from the six stations in the NEPL and its surroundings revealed large elevation-dependant variations in temperature. In Balochistan, the higher the station elevation, the lower the temperature(PMD, 2010). This relationship is displayed in Figure 6(b), which shows significant correlations (R^2: 0·84–0·94) between average daily maximum and minimum temperatures and station elevation. For modelling purposes, and to increase the accuracy of the SWAT-derived spatial distributions of precipitation (rain and snow), daily minimum and maximum temperatures were computed at fictitious stations using linear regressions with temperatures and elevations as variables. Data used in the regression analysis were extracted from the six temperature gauges (Figure 3(a), red crosses), four of which are located within the NEPL. The remaining two stations are from areas proximal to the NEPL. The elevations of these stations ranged from 1600 to 2400 m AMSL. The locations of the fictitious stations were distributed across the NEPL so as to provide a more or less even distribution, laterally and vertically, and temperatures at these fictitious stations (Figure 3(a),

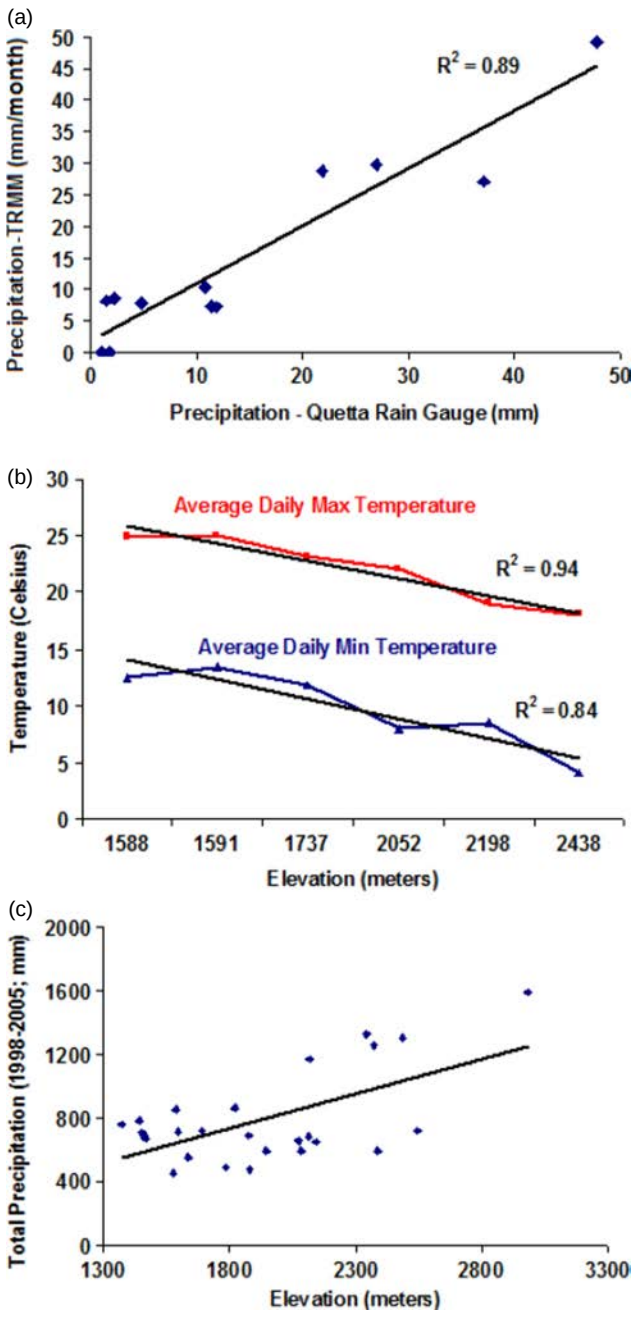

Figure 6. (a) Comparison between average monthly (1998–2005) precipitation reported from the Quetta Meteorological Station and TRMM-derived average monthly precipitation for the picture element covering the Quetta Meteorological Station. (b) Elevation-dependant variations in temperature revealed from a plot of average maximum and minimum temperatures extracted from six stations against their respective elevations. (c) Elevation-dependant variations in precipitation revealed from a plot of annual precipitation extracted for individual TRMM stations within NEPL against station elevation

black crosses) were estimated using regression relationships derived from daily temperature datasets.

Land use and soil types

Three major land use units were mapped throughout the watershed: agricultural, pasture, and mixed forest (Figure 3(a)), using the agricultural census land use data prepared by Pakistan's Agricultural Census Organization (ACO) and by the Agricultural Research Council of the Agricultural Department of Balochistan (Mirza, 1995; ACO, 2004). The highlands surrounding the Quetta Valley are largely composed of mixed forest and pasture, whereas the remaining lowlands are dominated by the agricultural and pasture land use types (Figures 1 and 3). Using the SWAT land use library, we selected the land use types that closely resemble the mapped units. For example, the mapped agricultural land use type was modelled as SWAT's AGRC–Agricultural Land-Close-grown. Similarly, mixed forest and pasture land use types were modelled as mixed forest and pasture, respectively, in SWAT.

Five main soil types were identified and mapped in the NEPL using published soil surveys (Abbas *et al*., 1987; HSC, 1961b; IIASES, 1992) (Figures 2 and 3(b)). These are: (i) alluvium, (ii) sandstone, (iii) shale, (iv) limestone (karstified or massive), and (v) metamorphic and igneous rocks. The saturated hydraulic conductivities for these soil types were extracted from published sources (IIASES, 1992; WAPDA, 2001; TCI *et al*., 2004). The reported range of hydraulic conductivities for the five soil types are as follows: alluvium, 28·8–324 mm/h; sandstone, 0·1–100 mm/h; limestone, 0·4–76 mm/h; shale 0·004–10 mm/h; and metamorphic and igneous rocks, 0·004–5 mm/h.

We compared the reported ranges for hydraulic conductivities for the five soil types in the study area to those listed (A: >7·6 mm/h; B: 3·8 to 7·6 mm/h; C: 1·3 to 3·8 mm/h; and D: 0·0 to 1·3 mm/h) for the SCS soil hydrologic groups (SCS, 1985) and classified them accordingly. The alluvium, sandstone, shale, massive limestone, karstified limestone, and metamorphic/igneous soil types were assigned to groups A, A, C, C, A, and D, respectively (Table I). Table I also lists the composition and age of the investigated lithologic units in the study area, their assigned soil types, and their reported hydraulic conductivities (HSC, 1961a; SCS, 1985; IIASES, 1992; Maidment, 1993; Kazmi *et al*., 2003; TCI *et al*., 2004).

Digital maps depicting distributions of soil hydrologic groups, together with the generated land use digital maps, were imported into the model and used to define multiple HRUs for each of the 104 sub-basins (Figure 5). With threshold levels of 20 and 10% for land use and soil, respectively, recommended by SWAT (DiLuzio *et al*., 2001), 4–12 HRUs were defined for each of 104 sub-basins, resulting in a total of 798 HRUs for the watershed. The integration of the information contained in the soil type and land use coverage allowed the extraction of CN distribution maps for each of the soil horizons across the entire watershed.

Model calibration and validation

Conventional calibration using stream flow data has limited application in our study area because only one flow gauge is available at Burj Aziz Khan Field Discharge Station in sub-basin 85 (IPD, 2006) (Figures 1 and 5). Because of the paucity of stream flow data, we

Table II. Significant calibration parameters (20 parameters) grouped in three main categories: snow, groundwater, and soil parameters

Parameter[a]	SWAT default range (value)	Final value	Definition
SFTMP	(−) 5–5 (1·0)[a,b]	−2·0	Snowfall temperature (°C)
SNOCOVMX	0–500 (1·0)[b]	500·0	Minimum snow water content that corresponds to 100% snow cover, SNO_{100} (mm H_2O)
SNO50COV	0–1 (0·5)[a]	0·5	Fraction of snow volume represented by SNOCOVMX that corresponds to 50% snow cover
TIMP	0–1 (1·0)[a]	1	Snow pack temperature lag factor
SMTMP	(−) 5–5 (0·5)[a]	3·0	Snow melt base temperature (°C)
SMFMX	0–10 (4·5)[c]	10	Melt factor for snow on June 21 (mm H_20/°C-day)
SMFMN	0–10 (4·5)[c]	0·0	Melt factor for snow on December 21 (mm H_20/°C-day)
SOL_AWC	Varies[a]	Varies (0·01–1)	Available water capacity of the soil layer (mm/mm soil)
ESCO	0–1 (0·95)[a]	0·0	Soil evaporation compensation factor
GWQMN	0–5000 (0)[a]	Varies (100–600)	Threshold depth of water in the shallow aquifer required for return flow to occur (mm H_2O)
REVAPMN	0–500 (1·0)[a]	500	Threshold depth of water in the shallow aquifer for 'revap' to occur (mm H2O)
GW_REVAP	0·2–1·0 (0·2)[a]	0·2	Groundwater 'revap' coefficient
GW_DELAY	0–500 (31)[e]	0	Groundwater delay time (days)
ALPHA_BF	0–1 (·048)[f]	Varies (0·048, 1)	Baseflow alpha factor (days)
RCHRG_DP	0–1 (0·05)[a]	0·05	Deep aquifer percolation fraction
CH_K1	0–150 (0·50)[g]	100·0	Effective hydraulic conductivity in tributary channel alluvium (mm/h)
CH_K2	0–150 (0·0)[g]	0·5	Effective hydraulic conductivity in main channel alluvium (mm/h)
CH_N1	0–0·3 (0·014)[h]	Varies (0·014)	Manning's '*n*' value for the tributary channels
CH_N2	0–0·3 (0·014)[h]	Varies (0·014)	Manning's '*n*' value for the main channel
RES_K	0–150 (0·50)[i]	Varies (5, 15)	Hydraulic conductivity of the reservoir bottom (mm/h)

[a] Neitsch *et al*. (2002), Maidment, Handbook of Hydrology (1993), TCI (2004).
[b] Anderson (1976).
[c] Huber and Dickinson (1988).
[d] USDA (1999).
[e] Sangrey *et al*. (1984).
[f] Smedema and Roycroft (1983).
[g] Lane (1983).
[h] Chow (1959).
[i] Halcrow and Cameous (2008), IIASES (1992), TCI (2004).

explored the utilisation of satellite data to improve model calibration. In addition to the traditional approaches to model calibration (e.g. manual and automatic calibrations, observed/simulated stream flow hydrographs), we developed methods that take advantage of observed changes in the volumes of the Khushdil Khan and Kara Lora reservoirs, which are located in sub-basins 21 and 44, respectively (Figure 5). The estimated reservoir storage was used as observational datasets for model calibration in addition to those observations at the outlet of the NEP. The adopted reservoir calibration method improved the model parameter adjustment given the rendered additional sources of observations and their wide spatial coverage. The satellite-based methodologies for estimating reservoir volumes were shown to be effective and of high precision (Peng *et al*., 2006).

Model calibration was conducted in three major steps via a stepwise, iterative process by adjusting the key snow pack/melt and soil/groundwater parameters. SWAT's default values were adopted as our initial parameter values, and the implemented adjustments were constrained by the ranges of parameter variation provided by SWAT. Table II defines the key parameters and lists the adopted value and SWAT's default value, range, and data source for each of them.

The first step is a coarse adjustment step for the snow pack/melt parameters (in a later section) for the entire watershed to calibrate the simulated flow rates with the observed peaks using the Burj Aziz Khan Field Discharge Station, which is located at the watershed outlet. Throughout the second step, we calibrated the simulated runoff reaching the Khushdil Khan and the Kara Lora reservoirs (sub-basins 21 and 44; Figure 5) against reservoir volumes extracted from temporal satellite imagery by adjusting key soil/groundwater parameters (in a later section). Since the two reservoir basins only amount to a smaller percentage of the watershed, the third step involved calibrating simulated flow against discharge flow from the Burj Aziz Khan Field Discharge Station for the remaining sub-basins by adjusting key soil/groundwater parameters and channel routing parameters, similar to adjustments made in step two (in a later section). Fine-tuning was then performed manually by repeating the calibration adjustments described

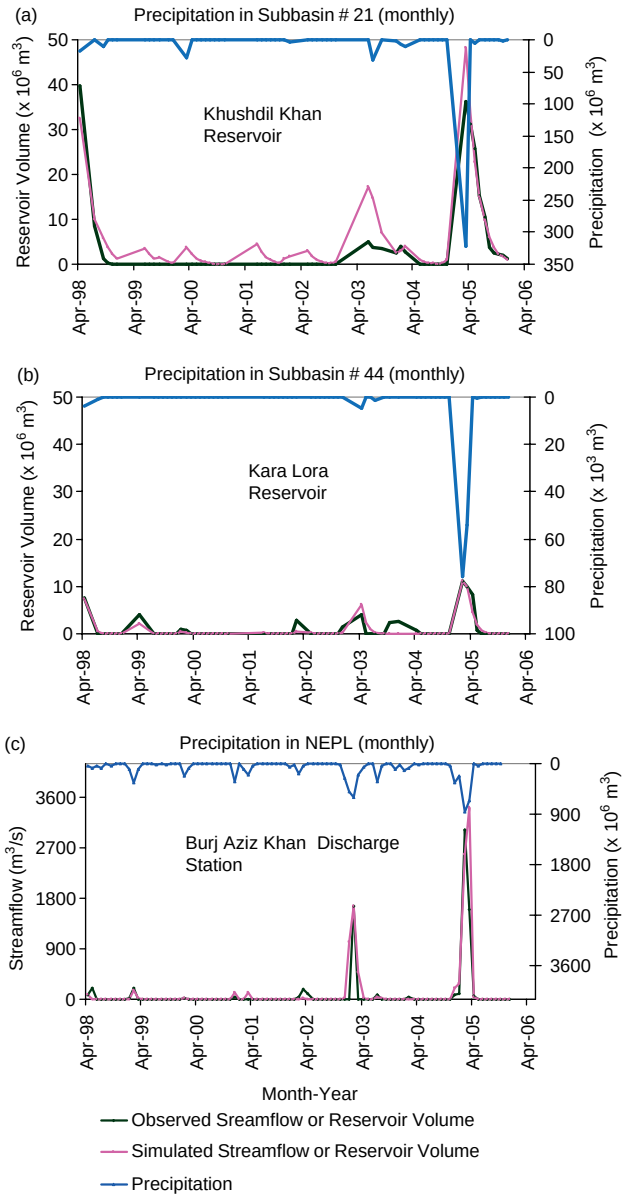

Figure 7. Time series calibration results (April 1998–December 2005). (a) Time series for the simulated and observed (from satellite data) reservoir volume for the Khushdil Khan Reservoir. (b) Time series for simulated and observed reservoir volume for the Kara Lora Reservoir. (c) Time series for simulated and observed stream flow at the Burj Aziz Khan station. Also shown are TRMM-derived monthly precipitation over sub-basin 21 (a), sub-basin 44 (b), and the NEPL watershed (c)

below until a best fit was achieved between modelled and observed reservoir volume and between modelled and observed flow values (Figure 7). The values for the parameters that achieved the optimum calibration are given in Table II.

Coarse adjustment and calibration of snowpack/melt parameters

Several main parameters related to snow formation/pack and melt were adjusted to calibrate the modelled flow rates against the observed peaks in the hydrographs. The SWAT model classifies precipitation as snow or rain depending on the mean daily air temperature (SFTMP). The observed peaks in the hydrographs coincided with the flooding periods in February and March, the snow melting period; the largest of these peaks occurred in 2003 and 2005 (Figure 7). The seasonal growth and recession of the snow pack was defined using an areal depletion curve (Anderson *et al.*, 1976). The snowmelt is constrained by the minimum snow water content that corresponds to 100% snow cover (SNOCOVMX) and a specified fraction of snow volume represented by SNOCOVMX that corresponds to 50% snow coverage (SNO50COV). Because of the lack of snow pack/melt data, we assumed a linear relationship for the depletion curve which was accomplished by assigning the SNO50COV a value corresponding to 50% of that of SNOCOVMX. The areal depletion curve affects snowmelt if the snow water content is below SNOCOVMX. In addition to the areal coverage of snow, snowmelt is also controlled by the snow pack temperature and melting rate. The former is influenced by a lagging factor (TIMP) and threshold temperature for snow melt (SMTMP). The melting rate is controlled by the maximum snowmelt factor (SMFMX) and the minimum snowmelt factor (SMFMN), estimated at 10 and 0, respectively, values that can account for the observed rapid snow melting during relatively short periods of time. The adjustments for the seven parameters (SFTMP, SNOCOVMX, SNO50COV, TIMP, SMTMP, SMFMX, and SMFMN) were made heuristically to achieve a general agreement between simulated and observed monthly hydrographs, particularly the large flood-induced peaks of 2003 and 2005. The characteristics of the simulated hydrograph were found to be more sensitive to the SNOCOVMX, SFTMP, and SMTMP parameters.

Delay action/storage dams and model calibration against reservoir volume and flow versus no-flow conditions in ephemeral streams

The next step in the calibration process was to calibrate the flows in two of the major sub-basins, taking advantage of the observed changes in reservoir volumes in these two areas. The reservoir volumes were calculated for each month using temporal Landsat scenes and SRTM data, except for the months during which reservoir areas were difficult to discern due to cloud coverage and/or poor-quality images. Reservoir volumes were calculated using the Three-Dimensional Analyst's Surface Volume Tool in ArcGIS 9·3.

The Landsat images were also used to extract first-order estimates of the reservoir storage parameters required for modelling reservoir storage and routing in SWAT. For the Khushdil Khan and Kara Lora reservoirs (Figure 5), these parameters include: (i) RES_PVOL, the volume of water that fills the reservoir to the principal spillway, assumed to be the volume of the reservoir at its largest observed areal extent and estimated at $53{\cdot}7 \times 10^6$ m^3 and 11×10^6 m^3 for the Khushdil Khan and Kara Lora reservoirs, respectively, (ii) RES_PSA, the surface area of the impounded water body that fills the reservoir to the principal spillway, assumed to be the largest

observed areal extent for the reservoir and estimated at $5{\cdot}2 \times 10^6$ m^2 and $0{\cdot}8 \times 10^6$ m^2, (iii) RES_EVOL, the volume of water that fills the reservoir to the emergency spillway, estimated at 59×10^6 m^3 and 12×10^6 m^3, and (iv) RES_ESA, the surface area of the impounded water that fills the reservoir to the emergency spillway, estimated at $5{\cdot}7 \times 10^6$ m^2 and $0{\cdot}9 \times 10^6$ m^2. Because RES_ESA has to be larger than RES_PSA, the former was estimated by multiplying the latter by an arbitrary multiplier (1·1). The same arbitrary multiplier was used to estimate RES_EVOL from RES-PVOL. Uncertainties in the satellite-derived monthly estimates of reservoir areas and volumes are difficult to ascertain, given that they are largely related to the absence of satellite data for a number of months throughout the investigated period. Additional uncertainties in reservoir volumes could arise from the differences in the spatial resolution of the images (SRTM: 90 m; TM: 30 m) that were utilized in reservoir volume extraction. The use of temporal satellite imagery for calibration purposes was not solely restricted to monitoring reservoir volumes; the images were also used to examine whether the main rivers were dry or wet (i.e. flowing or not flowing), and the model was calibrated to account for such types of observations.

Soil and groundwater parameters were adjusted to achieve finer fitting with estimated reservoir volumes. The groundwater parameters include soil available water capacity (SOL_AWC), soil evaporation compensation coefficient (ESCO), threshold water levels in shallow aquifer for base flow (GWQMN), re-evaporation/deep aquifer percolation (REVAPMN), re-evaporation coefficient (GW_REVAP), delay time for groundwater recharge (GW_DELAY), and base flow recession constant (ALPHA_BF). These parameters dictate the amount of water flow through the soil zone and underlying aquifer to the stream channel as well as the timing (Table II). The GWQMN, SOL_AWC, and hydraulic conductivity of reservoir bottom (CH_K) were found to be the major parameters affecting the reservoir volume.

Model calibration against stream flow data

The next step in the calibration process was to calibrate the modelled flow against the observed hydrograph at the Burji Aziz Khan station. All calibration parameters (Table II) were used for the calibration in this step with emphasis on those related to channel routing. Transmission losses through channels were calculated for both tributary and main channels. The key parameter for losses is the effective hydraulic conductivity (CH_K). Most tributary channels are ephemeral or intermittent, receiving little groundwater, and are thus likely to lose water to bank storage or to the underlying aquifer, whereas the main channels receive groundwater through lateral flow from soils, and thus the transmission losses for these channels are minimal (Lane, 1983). The initial hydraulic conductivity (CH_K1) values (0·5 mm/h) were adjusted (adopted value: 100·0 mm/h). A small transmission loss for the main channels was simulated by setting effective hydraulic conductivity (CH_K2) close to the SWAT default value (0·5 mm/h) (Table II).

Calibration criteria and model evaluation

The model parameters were adjusted in a SWAT domain using the procedures outlined above until the overall simulated values for stream flow were similar to the observed values. Two statistical measures, coefficient of determination (R^2) and coefficient of efficiency COE (Nash and Sutcliff, 1970), were used to quantify the achieved levels of calibration and evaluate the overall performance of the model. Figure 6 compares the simulated reservoir volumes to those extracted from satellite data, and simulated stream flow to observed stream flow over the calibration period (1998–2005). Visual inspection of Figure 6 shows a close agreement between simulated and observed monthly reservoir volumes and flow rates throughout the calibration period. High degrees of correlation were achieved between satellite-derived reservoir volumes and simulated reservoir volumes (R^2: 0·85 and 0·86; COE: 0·89 and 86; Figure 7), as well as a good correlation between observed and simulated stream flow values at the watershed outlet (R^2: 0·78, COE: 0·69; Figure 7).

DISCUSSION AND RESULTS

Novelty of model

The NEPL, like the majority of the world's basins, lacks adequate field data for the construction and calibration of reliable rainfall-runoff models. With daily precipitation extracted from a single precipitation gauge (Quetta Station) in the NEPL, and with simulated flows calibrated against stream flow from the only gauge at the outlet of the watershed, any constructed rainfall-runoff model for the basin will undoubtedly yield unreliable, and most likely fictitious, results. Because of the lack of adequate field data in the NEPL, previous attempts (e.g. WAPDA, 2001; Shan *et al.*, 2002; Kazmi *et al.*, 2003; TCI *et al.*, 2004) to assess water resources in the NEPL in particular, and the Pishin Lora basin in general, were based largely on simplified water balance calculations in which evapotranspiration, runoff, and groundwater recharge were extracted locally from limited observations from few field gauging stations in the Quetta Valley and the surrounding area. The uncertainties associated with such water-balance calculations in the NEPL basin and its surroundings are reflected in the large variations in the reported mean annual rainfall (150–300 mm/year, or 1·3–2·6 10^9 m^3/year) and in the estimated partitioning of the rainfall into runoff (5–20%), evapotranspiration (38–78%), and infiltration/recharge (20–40%) (e.g. WAPDA, 2001; Shan *et al.*, 2002; Kazmi *et al.*, 2003; TCI *et al.*, 2004). The results from such studies should be regarded with caution because of the extreme temporal and spatial variability in precipitation, surface water,

and the hydrologic parameters across the examined area (Kazmi *et al*., 2003; Tareen *et al*., 2008).

Our approach addresses these problems by complementing the limited existing field data with observations derived from readily available remote sensing datasets. The remote sensing data are used as input to the model and for calibration purposes. Precipitation was derived from TRMM data covering the entire NEPL area and surroundings with 36 picture elements (i.e. stations; Figure 4(a)). Earlier studies (Turk *et al*., 2003; Chiu *et al*., 2006; Chokngamwong and Chiu, 2006; Milewski *et al*., 2009a;) cautioned against uncertainties in TRMM-derived precipitation, but our comparisons showed a good correspondence (R^2: 0·89; Figure 6(a)) between precipitation from the Quetta rain gauge and that derived from TRMM data over the same area.

The use of satellite-based precipitation data provided adequate spatial coverage with uninterrupted data for some eight years and captured topography-related variations in precipitation in the area. It has been shown in many mountainous areas worldwide that precipitation over the mountains far exceeds that in the surrounding valleys (Saudi Arabia: Sorman and Abdulrazzak, 1993; Death Valley: Osterkamp *et al*., 1994). Similar trends were observed in the study area; a positive correlation is observed between the average elevation and TRMM-derived average annual (1998–2005) precipitation over the Takhatu mountain ranges and the surrounding valleys and lowlands (Figures 1 and 6(c)). The average annual TRMM-derived precipitation over the NEPL is 155 mm/year, or $1{\cdot}31 \times 10^9$ m^3/year, approximately 30% more than the estimates (125 mm/year, or $1{\cdot}06 \times 10^9$ m^3/year) that assume the same reported precipitation from the Quetta station across the entire NEPL basin.

Average annual precipitation for the NE, NW, and southern basins of the NEPL were estimated from TRMM data at 194 mm/year (570×10^6 m^3), 134 mm/year (320×10^6 m^3), and 124 mm/year (390×10^6 m^3), respectively (Figure 8(c); Table III). As expected, the NE basin, which has the highest elevation (average elevation: 2700 m AMSL), receives the highest amount of

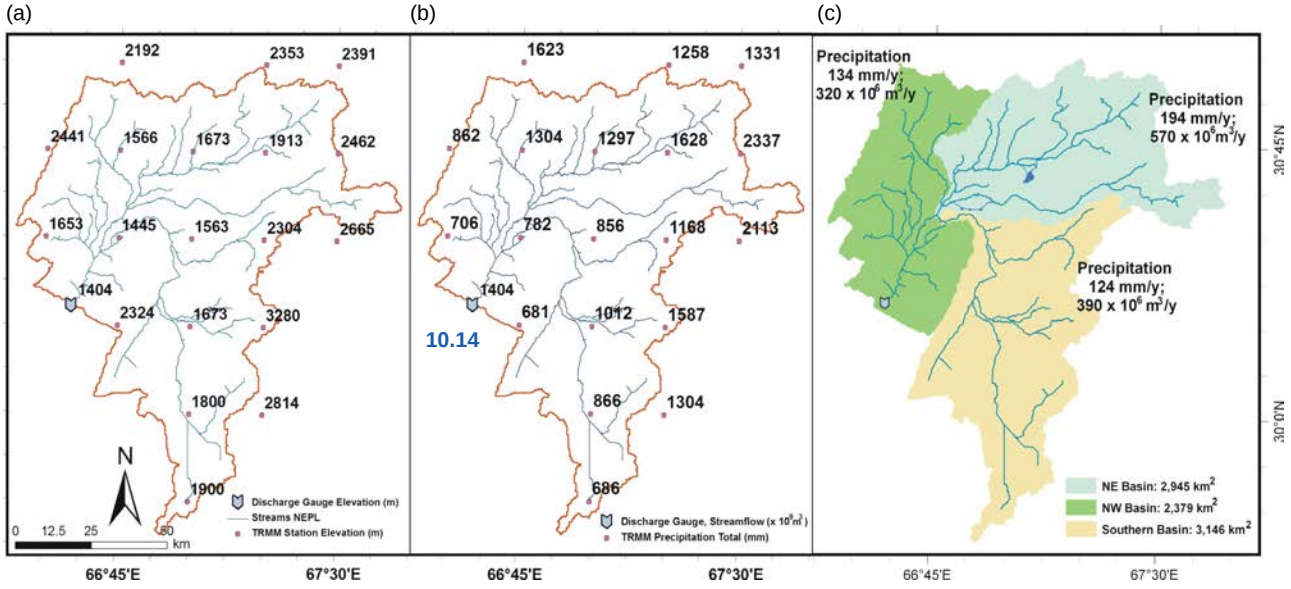

Figure 8. Precipitation and elevation for TRMM stations in the NEPL and its major basins. (a) Elevations for each of the TRMM picture elements within NEPL measured at its centre. (b) Cumulative precipitation (1998–2005) for each of the TRMM stations within NEPL. Also shown is the cumulative simulated stream flow for the same duration at the Burj Aziz Khan station. (c) Average Annual TRMM precipitation over the three major basins in the NEPL, namely the NE, NW, and southern basins

Table III. Modelled average annual (1998–2005) values of hydrologic variables for the NEPL watershed and its three major basins (NE, NW, and southern basins)

Basin	Basin area		Annual precipitation depth	Annual precipitation volume		ET		Recharge		Runoff	
	km^2	(%) of NEPL	mm/y	$\times 10^6$ m^3/y	Basin precip (%)	$\times 10^6$ m^3/y	Precip (%)	$\times 10^6$ m^3/y	Precip (%)	$\times 10^6$ m^3/y	Precip (%)
NE	2,945	35	194	571	45	364	64	172	30	38	7
NW	2,379	28	134	320	25	208	65	84	26	26	8
Southern	3,146	37	124	389	30	275	71	105	27	8	2
NEPL	8,470	100	151	1,280	100	847	66	361	28	72	6

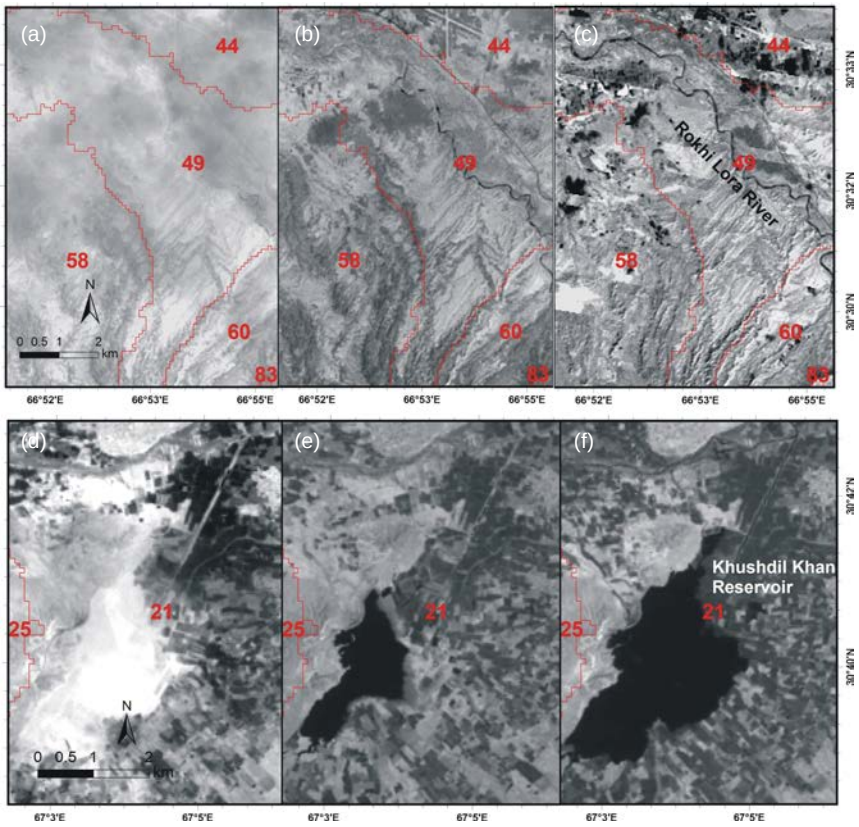

Figure 9. Temporal Landsat band 5 images over the ephemeral Rokhi Lora River and the Khushdil Khan reservoir under flowing and non-flowing conditions. In wet periods, streams appear as dark lines ((b), (c)) and reservoirs filled by impounded waters appear as dark polygons ((e), (f)), whereas in dry periods streams and reservoirs appear in bright shades, making them indistinguishable from their surroundings ((a), (d))

precipitation; the southern basin, the basin with the lowest elevation (average elevation: 1600 m AMSL), receives the least amount of precipitation; and the NW basin, with intermediate average elevation (average elevation: 2200 m AMSL), receives intermediate amounts of precipitation (Figures 1, 4(i), and 8).

Calibrating each of the basins is an important step toward the calibration of the entire watershed. To compensate for the lack of adequate stream flow gauge data coverage for the NEPL, we took advantage of temporal changes in the areal extent of the reservoirs—such as those observed on temporal satellite imagery for the months of March 2000 (Figure 9(d)), March 2003 (Figure 9(e)), and March 2005 (Figure 9(f))—to calibrate the simulated flow. The estimated volumes of impounded water for these three periods are 0·0 m^3, $7{\cdot}2 \times 10^6$ m^3, and $53{\cdot}7 \times 10^6$ m^3, respectively. The use of temporal satellite imagery for calibration purposes was not solely restricted to monitoring the temporal variations in reservoir volumes, but the images were also used to examine whether the main rivers were dry or wet. For example, our examination of cloud-free, temporal satellite images (64 images; one to two images/month on average) acquired over the Rokhi Lora River at the outlet of the southern sub-basin 49 (Figures 3(b) and 5) between 1998 and 2005 indicated that the river remained dry throughout the examined period except in the springs of 2003 and 2005 (Figures 9(b) and 9(c)). These observations were accounted for in the calibrated model. The calibrated model yielded no flow at this location except for the months of February and March in 2003, when the simulated flow was 39·8 and 19·4 m^3/s, and in the months of February, March, and April 2005, when the simulated flow was 58·8, 114·1, and 7·4 m^3/s, respectively. Similar observations that pertain to the presence or absence of water in the main ephemeral streams across the NEPL watershed throughout the calibration period were made from temporal satellite data and used to calibrate the model as described above.

Model applications

The calibrated model serves a number of purposes, the most important of which include: (i) providing an understanding for the spatial and temporal partitioning of precipitation into runoff, recharge, and evapotranspiration, and (ii) utilising the model to simulate various water management scenarios. In Table III, we provide model results for the entire basin and for each of the three major basins within the NEPL watershed, namely the NE, NW, and southern basins (Figures 1, 4(i), and 5), to better understand spatial variations in the partitioning of precipitation from one part to another in the NEPL. Such an understanding is needed as we use the calibrated model to examine various potential scenarios for water management across the NEPL.

The average annual precipitation ($1,280 \times 10^6$ m^3; 151·1 mm/year) in the NEPL (Table III) is partitioned as follows: (i) runoff is estimated at the Burji Aziz

Khan station at 72×10^6 m^3/year (6% total precipitation), (ii) recharge is estimated at 361×10^6 m^3/year (28% total precipitation), and (iii) evapotranspiration (initial losses) estimated at 847×10^6 m^3/year (66% total precipitation). The recharge reported in Table IV includes contributions from transmission losses ($22{\cdot}8 \times 10^6$ m^3/year; 2% total precipitation), reservoir seepage ($74{\cdot}6 \times 10^6$ m^3/year; 6% total precipitation), percolation out of soil (280×10^6 m^3/year; 22% total precipitation), and water moving out of the soil (16×10^6 m^3/year; 1%). Unlike ours, earlier attempts did not fully account for large variability (of precipitation, elevation, hydrologic properties, etc.) across the watershed.

As described earlier, the highest precipitation rates are observed in the NE basin (194·0 mm/year), the lowest were observed in the southern basin (123·6 mm/year), and intermediate values (134·3 mm) were observed over the NW basin (Figure 8(c); Table III). The southern basin receives the lowest amount of precipitation and is largely covered by alluvial deposits (50·3% of total area) and karstified limestone (29·3% of total area) (Figure 3(b)). These features could explain the reduced runoff in the southern basin compared to the NW and NE basins (NW runoff: $26{\cdot}4 \times 10^6$ m^3/year; NE runoff: $37{\cdot}8 \times 10^6$ m^3/year; South runoff: $7{\cdot}7 \times 10^6$ m^3/year). The northern sections of the NW basin on the other hand, are largely covered (23·3% of total area) by outcrops of shale, a rock type that promotes runoff and inhibits recharge (Figure 3(b)). Indeed, the NE basin has the highest runoff ($37{\cdot}8 \times 10^6$ m^3/year), followed by the NW basin ($26{\cdot}4 \times 10^6$ m^3/year). The NE basin experiences the largest amounts and proportions of recharge (172×10^6 m^3/year) compared to the NW (84×10^6 m^3/year) and southern basins (105×10^6 m^3/year). This is largely related to the infiltration of the runoff impounded behind the two major reservoirs and the presence of extensive outcrops of alluvial deposits (34·2% of total area) and sandstone (52·8%) that facilitate infiltration within the basin (Figure 3(b)).

The position of the two reservoirs, the Khushdil Khan and the Kara Lora (Figure 5), were carefully selected; they collect runoff from watersheds that cover a large area (Khushdil Khan: 1320 km^2; Kara Lora: 960 km^2), with source areas that receive large amounts of precipitation in the high Takhatu mountain range (Figure 1). Runoff at the dam locations is substantial; using the calibrated model, we estimate that the average annual (1998–2005) stream flows at Khushdil Khan and Kara Lora are 65×10^6 m^3, and 35×10^6 m^3, respectively. Moreover, the reservoirs are floored by thick (up to 900 m) and extensive alluvial deposits that enhance recharge (Kazmi *et al*., 2003; TCI *et al*., 2004).

The delay action dams were constructed for one main purpose, to increase infiltration. Currently, water consumption in the NEPL is about 400×10^6 m^3/year (TCI *et al*., 2004; Halcrow and Cameous, 2008), which exceeds our estimates for recharge (361×10^6 m^3/year; Table III), even with the Khushdil Khan and the Kara Lora reservoirs in place. The difference is substantial, approximately 40×10^6 m^3/year. Currently, population is concentrated in the southern part of the NEPL, and so are the delay action dams; over 100 small dams were constructed in the southern basin of the NEPL (Halcrow and Cameous, 2008). The concentration of the population in the southern basin and the reduced precipitation in this area contributed to the reduced runoff from the southern basin (Table III). No additional delay action dams are proposed in the southern basin; instead, we suggest that such dams be created in the NE and NW basins. Using criteria similar to those noted above for the Khushdil Khan and Kara Lora reservoirs, we suggest three locations for the construction of delay action dams, two in the NW basin and a third in the NE basin (Figure 5). One of the two proposed dams (reservoir 1) in the NW basin is on the Arambi Manda River (Figures 3(b) and 5) at the outlet of sub-basin 40 and the other (reservoir 2) is on the outlet of sub-basin 68. The latter impounds runoff from the Loe Kandil Chul and the Loe Dara Rivers (Figures 3(b) and 5). The size of the drained sub-basins is large (reservoir 1: 620 km^2; reservoir 2: 940 km^2); their source areas are in the surrounding Takhatu mountain range, which receives substantial precipitation. The average annual runoff impounded by the dams is large (reservoir 1: 14×10^6 km^3; reservoir 2: 10×10^6 km^3), and the area over which the reservoir will be developed is covered by thick (up to 900 m) alluvium with high infiltration rates (Kazmi *et al*., 2003; TCI *et al*., 2004).

Despite the fact that two major reservoirs were constructed on the NE basin and a considerable fraction of the recharge in this basin is attributed to the construction of the two dams, the runoff at the outlet of the NE basin is still the highest ($37{\cdot}8 \times 10^6$ m^3) of the three basins (Table III). We propose an additional reservoir (reservoir 3) at the outlet of sub-basin 41 (Figure 5). The size of the drained area is large (720 km^2; Figure 5); its source area is in the Takhatu mountain range, with elevations reaching up to 4000 m AMSL (Figure 1) and precipitation rates of up to 700 mm/year (Figure 4). As is the case with all the existing and suggested dam locations, alluvial deposits are widespread (34% of the NE basin) and thick (up to 900 m) (Kazmi *et al*., 2003; TCI *et al*., 2004).

Three scenarios were considered. The first calls for the construction of reservoirs 1 and 2, the second for the construction of reservoir 3, and the third for the construction of reservoirs 1, 2, and 3 (Figure 5). Reservoir parameters were assumed to be similar to those assigned for the existing reservoir in sub-basin 21 (Figure 5). The results of these simulations are given in Table IV. The table shows a progressive increase in reservoir seepage and recharge for scenarios 1 through 3 (scenario 1: 107×10^6 m^3/year, 393×10^6 m^3/year; scenario 2: 120×10^6 m^3/year, 404×10^6 m^3/year; and scenario 3: 155×10^6 m^3/year, 432×10^6 m^3/year). If we were to implement scenarios 1, 2, or 3, we could achieve sustainable to near-sustainable systems in which the recharge ($393–432 \times 10^6$ m^3/year; Table IV) approximates or exceeds consumption (400×10^6 m^3/year) (TCI

Table IV. Scenarios for increasing recharge by constructing reservoirs

Proposed delay action dams		Average annual recharge		Stream flow	
Scenarios	Location	Net recharge		Runoff on Burj Aziz Khan discharge station	
		$\times 10^6$ m^3/y	%	$\times 10^6$ m^3/y	%
1: Reservoirs 1 and 2	Sub-basins # 40, # 68	393	31	47	4
2: Reservoir 3	Sub-basin # 41	404	32	37	3
3: Reservoirs 1, 2 and 3	Sub-basin # 40, 68, 41	432	34	8·5	1

et al., 2004; Halcrow and Cameous, 2008). This would come at the expense of decreased runoff at the Burji Aziz Khan station. Annual flow is estimated to decrease from 72×10^6 m^3/year to 47×10^6 m^3/year with the implementation of scenario 1. If scenarios 2 and 3 were to be implemented, the flow will be reduced to 37×10^6 m^3/year, and $8{\cdot}5 \times 10^6$ m^3/year, respectively. A cost-effective alternative to the construction of a limited number of large dams (e.g. reservoirs 1, 2, and 3) would be to develop tens of smaller delay action dams in the NE and NW basins over areas covered by alluvial deposits. Such small dams could be constructed in the NW basin in sub-basins 23, 40, 48, 54, 56, 57, 61, 62, and 68 and in the NE basin in sub-basins 25, 28, 29, 31, 33, 41 (Figure 5).

SUMMARY

The NE part of Pishin Lora (NEPL) is one of the poorest and most disadvantaged provinces in Balochistan. It is currently facing severe water shortages that are largely related to migration from neighbouring war-infested Afghanistan and drought-related population migration from the rural areas to urban centres. Given the difficulty of accessing the region and the paucity of field data, we adopted methodologies that rely heavily on readily available remote sensing technologies as viable alternatives and useful tools for the assessment and management of the water resources of these remote regions. We adopted a catchment-based continuous (1998–2005) rainfall-runoff model for the NEPL watershed and calibrated the model against stream flow data and observations extracted from temporal satellite imagery. Inputs to the model included satellite-based 3-hourly TRMM precipitation data, and modelled runoff was calibrated against (i) estimates of water volumes impounded behind the Khushdil Khan and the Kara Lora reservoirs, where the reservoir volumes were extracted from digital topography and temporal satellite images, and (ii) satellite-based observations pertaining to the presence or absence of water in streams across the NEPL within the investigated period. Finally, the simulated runoff at the outlet of the watershed was calibrated against observed flow as reported from the Burj Aziz Khan station.

Using the calibrated model, the average annual precipitation (1998–2005), runoff, and recharge were estimated at 1300×10^6 m^3, 148×10^6 m^3, and 361×10^6 m^3, respectively. The calibrated model was also used to characterize the spatial and temporal variations in water partitioning within the various basins, namely the NE, NW, and southern basins. The highest precipitation rates (194 mm/year) and runoff ($37{\cdot}8 \times 10^6$ m^3/year) are in the NE basin, and the lowest rates (123·6 mm/year) and runoff ($7{\cdot}7 \times 10^6$ m^3/year) in the southern basin, whereas the NW basin experiences intermediate precipitation rates (134·3 mm/year) and runoff values ($26{\cdot}4 \times 10^6$ m^3/year). The calibrated model was also used to examine scenarios for sustainable management of the water resources of the NEPL. Results indicate that the construction of delay action dams in the NE and NW basins of the NEPL could increase recharge from 361×10^6 m^3/year to up to 432×10^6 m^3/year and achieve sustainable extraction.

The developed methodologies can be applied to many parts of the less-studied watersheds of the world, especially in areas where field data is inadequate and accessibility is limited. One of the main features of our methodology is the utilisation of global datasets that are readily available for most of the world's land surface. The adopted methodologies are not a substitute for traditional approaches that require extensive field datasets, but they could provide first-order estimates for rainfall, runoff, and recharge over large areas that lack adequate coverage with stream flow and precipitation data.

ACKNOWLEDGEMENTS

Funding was provided by the US Agency for International Development, in cooperation with the Higher Education Commission of Pakistan.

REFERENCES

Abbas G, Mureed S, Saris M, Ahmad S, Mehmood S. 1987. *Urban Geologic Map of Pakistan, Balochistan series*. Scale 1 : 100000. In *Geological Survey of Pakistan*, Quetta.

ACO. 2004. *Agriculture Census 2002: Landuse in Balochistan*, Agricultural Department: Balochistan, Pakistan.

Aftab S. 1997. Hydrogeology and groundwater resources of Balochistan, Pakistan; an overview. *Acta Mineralogica Pakistanica* **8**: 30–38.

Anderson JR, Hardy EE, Roach JT, Witmer RE. 1976. A land use and land cover classification system for use with remote sensor data. *U.S. Geological Survey Professional Paper* 964: p. 28.

Arnold JG, Fohrer N. 2005. Current Capabilities and Research Opportunities in Applied Watershed Modeling. *Hydrological Processes* **19**: 563–572.

Arnold JG, Srinisvan R, Muttiah RS, Williams JR. 1998. Large Area Hydrologic Modeling and Assessment, Part I: Model Development. *Journal of American Water Resource Association* **34**(1): 73–89.

Chiu L, Liu Z, Vongsaard J, Morain S, Budge A, Neville P, Bales C. 2006. Comparison of TRMM and Water District Rain Rates over New Mexico. *Advances in Atmospheric Sciences* **23**(1): 1–13.

Chokngamwong R, Chiu L. 2006. TRMM and Thailand Daily Gauge Rainfall Comparison, *American Meteorological Society* Atlanta, Georgia, p. 10.

Chow VT. 1959. *Open Channel Hydraulics* McGraw-Hill Inc.: New York.

DiLuzio M, Srinivasan R, Arnold JG, Neitsch SL. 2001. *Arcview Interface for SWAT2000 User's Guide*. US Department of Agriculture-Agricultural Research Service: Temple, TX.

Droogers P, Bastiaanssen W. 2002. Irrigation Performance Using Hydrological Modelling and Remote Sensing. *Journal of Irrigation Drainage Engineers* **128**(1): 11–18.

Garbrecht J, Martz L. 1995. TOPAZ: An Automated Digital Landscape Analysis Tool for Topographic Evaluation, Drainage Identification, Watershed Segmentation, and Sub-Catchment Parameterization: Overview. *Agricultural Research Service NAWQL* **95**(1).

Halcrow Cameous. 2008. Halcrow and Cameous Consultant Companies. Effectiveness of the Delay Action/Storage Dams in Balochistan. *TA-4560(PAK) Project, Asian Development Bank*, Quetta.

HSC. 1961a. Hunting Survey Corporation. Reconnaissance Geology of part of West Pakistan, Balochistan, *A Colombo Plan cooperative project*, Toronto (A report published for the Government of Pakistan by the Government of Canada).

HSC. 1961b. Hunting Survey Corporation. Reconnaissance Geology of part of West Pakistan, Geologic Map series. Scale 1 : 253440. In: (Gov. of Canada) *A Colombo Plan cooperative project*, Toronto (A report published for the Government of Pakistan by the Government of Canada).

Huber WC, Dickinson RE. 1988. *Storm water management model, version 4: user's manual*, Athens, GA.

IIASES. 1992. International Institute for Aerospace Survey and Earth Sciences. *Soil Survey of Pakistan.* Land Resources and Urban Sciences Department, Balochistan, Quetta.

IPD. 2006. Irrigation and Power Department. Assessment of Water Resources Availability and Water Use for Balochistan, *Stream Gauges database*, Government of Balochistan: Quetta.

IWRM. 2004. Integrated Water Resources Management. *Balochistan Resource Management Programme, Balochistan, Pakistan*. September 2004, component #3, Quetta.

Kazmi AH, Abbas G, Younas S. 2003. Water Resources and Hydrogeology of Quetta Basin, Balochistan, Pakistan. *Geological Survey of Pakistan*, Quetta.

Lane LJ. 1983. Chapter 19: Transmission Losses, in *SCS—National Engineering Handbook, Section 4: Hydrology*. U.S. Government Printing Office: Washington, DC, pp. 19·1–19·21.

Maidment DR. 1993. *Handbook of Hydrology* McGraw-Hill: Austin, TX.

Majeed Z, Khan AI. 2008. Dam failures due to flash floods and it's review for Mirani Dam project. *Water and Power Development Authority, Balochistan*, Quetta, pp. 1–10.

Milewski A, Sultan M, Yan E, Becker R, Abdeldayem A, Soliman F, Abdel Gelil K. 2009a. A remote sensing solution for estimating runoff and recharge in arid environments. *Journal of Hydrology* **373**: 1–14.

Milewski A, Sultan M, Jayaprakash SM, Balekai R, Becker R. 2009b. RESDEM, a tool for integrating temporal remote sensing data for use in hydrogeologic investigations. *Computers & Geosciences* **35**(10): 2001–2010.

Miller S, Kepner W, Mehaffey M, Hernandez M, Miller R, Goodrich D, Devonald K, Heggem D, Miller P. 2002. Integrating Landscape Assessment and Hydrologic Modeling for Land Cover Change Analysis. *Journal of the American Water Resources Associate* **38**: 915–929.

Mirza SN. 1995. Four wing saltbush—A multipurpose shrub for arid highlands of Balochistan. *Arid zone Research Institute*, Pakistan Agricultural Research Council, Quetta, pp. 1–18.

Monteith JL. 1981. Evaporation and Surface Temperature. *Quarterly Journal of the Royal Meteorological Society* **10**(451): 1–27.

Nash JE, Sutcliff JV. 1970. River flow forecasting through conceptual models. Part-1 a discussion of principles. *Journal of Hydrology* **10**: 282–290.

Neitsch SL, Arnold JG, Kiniry JR, Srinivasan R, Williams JR. 2002. Soil and Water Assessment Tool: User Manual, Version 2000, Grassland, *Soil and Water Research Laboratory* Temple, TX.

Osterkamp W, Lane L, Savard C. 1994. Recharge Estimates Using A Geomorphic Distributed-Parameter Simulation Approach. *Amargosa River Basin* **30**(3): 493–507.

Ottle C, Vidal-Madjar D, Girard G. 1989. Remote Sensing Applications to Hydrological Modeling. *Journal of Hydrology* **105**: 369–384.

Peng D, Guo S, Liu P, Liu T. 2006. Reservoir Storage Curve Estimation Based on Remote Sensing Data. *Journal of Hydrologic Engineering* **11**(2): 165–172.

PMD. 2010. Pakistan Meteorological Department. Climate Data: Daily Temperature in Balochistan, in *Climate Data Processing Centre*, Quetta, http://pakmet.com.pk.

RedCross. 2005. Pakistan: floods in Balochistan. Information bulletin # 1, February 2005, Pakistan Red Crescent Society, *Federation's Disaster Relief Emergency Group*, Quetta, http://ifrc.org.

Sangrey DA, Harrop-Williams KO, Klaiber JA. 1984. Predicting groundwater response to precipitation. *ASCE Journal of Geotechnical Engineering* **110**(7): 957–975.

Schultz GA. 1993. Hydrological Modeling Based on Remote Sensing Information. *Advances in Space Research* **13**: 149–166.

SCS. 1972. Soil Conservation Service. *Section 4: Hydrology, National Engineering Handbook*. U.S. Department of Agriculture, Engineering Division: Washington, DC, USA.

SCS. 1985. Soil Conservation Service. *Section 4: Hydrology, National Engineering Handbook*. US Department of Agriculture, Engineering Division: Washington, DC, USA.

Shan SHA. 1972. The geological structure as a guide in search for ground water in higher region of Balochistan. *Geonews, Geological Survey of Pakistan*, **2**(2): 21–22.

Shan XJ, Song XY, Liu JH, Wang CL. 2002. Obtaining digital elevation data in different terrain and physiognomy regions with spaceborne InSAR and its application analysis. *Chinese Science Bulletin* **47**(10): 868–873.

Simpson J, Adler RF, North GR. 1988. Proposed Tropical Rainfall Measuring Mission (TRMM) Satellite. *Bulletin of American Meteorological Society* **69**: 278–295.

Smedema LK, Roycroft DW. 1983. *Land drainage—planning and design of agricultural drainage systems*, Cornell University Press: Ithaca, New York.

Sorman AU, Abdulrazzak MJ. 1993. Infiltration-Recharge through Wadi Beds in Arid Regions. *Hydrological Sciences Journal-Journal Des Sciences Hydrologiques* **38**(3): 173–186.

Srinivasan R, Ramanarayanan TS, Arnold JG, Bednarz ST. 1998. Large area hydrologic modeling and assessment. Part II: model application. *Journal of American Water Resource Association* **34**(1): 91–101.

Tareen S, Sani B, Babar K, Ahmad S. 2008. Re-assessment of Water Resource Availability and Use for the Major River Basins of Balochistan—Study Findings, Policy Issues and Reforms. *Water for Balochistan* **4**(7).

TCI, Cameous, ARD. 2004. Techno Consult International Corporation, Cameous and Arab Resources Development. Research for water and sanitation authority, Quetta. *Quetta water supply and environmental improvement project.* 2008/2.

Treloar PJ, Izatt CN. 1993. Tectonics of the Himalayan collision between the Indian Plate and the Afghan Block—A synthesis. In *Geological Society Special Publications* (Treloar PJ, Searle MP (eds), *Himalayan tectonics*: 69–87.

Turk J, Eber E, Oh HJ, Sohn BJ, Levizzani V, Smith E, Ferraro R. 2003. Validation of an Operational Global Precipitation Analysis at Short Time Scales, *12th Conference on Satellite Meteorology and Oceanography*, and *3rd Conference on Artificial Intelligence Applications to Environmental Science*, Seattle, Washington.

USDA, NRCS. 1999. US Department of Agriculture, Natural Resources Conservation Service. *Soil Taxonomy: A Basic System of Soil Classification for Making and Interpreting Soil Surveys.*

WAPDA. 2001. Water and Power Development Authority. *Individual Basinal Reports of Balochistan, Hydrogeology Project*, Quetta, 1982–2000, Pakistan, Water and Power Development Authority, Pakistan, Quetta.

